

## TECHNICAL REPORTS

## Trace Elements in the Environment

# Mercury dynamics in the pore water of peat columns during experimental freezing and thawing

Jennie I. Sirota<sup>1</sup>  | Randall K. Kolka<sup>2</sup>  | Stephen D. Sebestyen<sup>2</sup>  | Edward A. Nater<sup>3</sup>

<sup>1</sup>Dep. of Forest Resources, Univ. of Minnesota, 1530 Cleveland Ave. N, St. Paul, MN 55108

<sup>2</sup>Northern Research Station, USDA Forest Service, 1831 Hwy 169 East, Grand Rapids, MN 55744

<sup>3</sup>Dep. of Soil, Water, and Climate, Univ. of Minnesota, 1991 Upper Buford Circle, St. Paul, MN 55108

## Correspondence

Jennie I. Sirota, Dep. of Forest Resources, Univ. of Minnesota, 1530 Cleveland Ave. N, St. Paul, MN 55108.

Email: siro0033@umn.edu

## Funding information

USDA Forest Service Northern Research Station

Assigned to Associate Editor Diederik Jacques.

## Abstract

Biogeochemical processes in northern peatland ecosystems are influenced by seasonal temperature fluctuations that are changing with the climate. Methylmercury (MeHg), commonly produced in peatlands, affects downstream waters; therefore, it is important to understand how temperature transitions affect mercury (Hg) dynamics. We investigated how the freeze–thaw cycle influences belowground peat pore water total Hg (THg), MeHg, and dissolved organic carbon (DOC). Four large, intact peat columns were removed from an ombrotrophic peat bog and experimentally frozen and thawed. Pore water was sampled across seven depths in the peat columns during the freeze–thaw cycle and analyzed for THg, MeHg, and DOC concentrations. Freezing results showed increased concentrations of THg below the ice layers and limited change in MeHg concentrations. During thawing, THg concentrations significantly increased, whereas MeHg concentrations decreased. Limited bromide movement and depth decreases in THg and DOC concentrations were associated with increased bulk density and degree of humification in the peat. The experiment demonstrates the effects of the freeze–thaw cycle on Hg concentrations in northern peatlands. Changes to freeze–thaw cycles with climate change may exacerbate Hg cycling and transport processes in peatland environments.

## 1 | INTRODUCTION

Mercury (Hg) is a global pollutant that is deposited from the atmosphere onto terrestrial environments, including peatlands (Kolka, Nater, Grigal, & Verry, 1999b; Kolka et al., 2011). Mercury has an extremely strong affinity for binding sites on organic matter (Skylberg, Xia, Bloom, Nater, & Bleam, 2000; Xia et al., 1999) and dissolved organic carbon (DOC) (Driscoll et al., 1995) in peatland soils. Consequently, peatlands can store large quantities of Hg relative to upland

mineral soils (Kolka, Grigal, Nater, & Verry, 2001; Kolka et al., 2011).

Inorganic Hg in peatlands can undergo methylation, where Hg is converted into the highly toxic and bioavailable form monomethylmercury ( $\text{HgCH}_3^+$ , commonly called methylmercury and abbreviated as MeHg) (Kolka et al., 2011; Morel, Kraepiel, & Amyot, 1998). Methylmercury is the most toxic form of Hg found in the environment and can bioaccumulate in fish, animals, and humans that consume aquatic organisms (Driscoll, Mason, Chan, Jacob, & Pirrone, 2013). Mercury methylation is mediated, in part, by anaerobic bacteria (e.g., sulfate-reducing bacteria) that convert Hg to MeHg (Branfireun, Roulet, Kelly, & Rudd, 1999; Gilmour & Henry, 1991; Jones et al., 2019). Temperature is also an important factor in this process (Celo, Lean, & Scott, 2006): warmer

**Abbreviations:** DOC, dissolved organic carbon; MEF, Marcell Experimental Forest; MeHg, methylmercury; PFA, perfluoroalkoxy; RPD, relative percent difference; THg, total mercury.

conditions lead to faster sulfate reduction (Sokolova, 2010) and presumably higher rates of Hg methylation.

The freeze–thaw cycle is an abiotic disturbance that can cause physical and chemical changes in soil (Hodgkins et al., 2014; Matzner & Borken, 2008; Yu, 2013) and influence soil processes (Corbett-Hains, Walters, & Van Heyst, 2012). In soils with high water content, such as peatlands, freezing can lead to concrete frost formation where both the water and soil freeze solid (Trimble, Sartz, & Pierce, 1958; Verry, 1991). Hydrogen bonds between water molecules exclude solutes from ice crystals during the onset of freezing (Corte, 1962; Kadlec, 1984; Verry, 1991; Verry, Brooks, Nichols, Ferris, & Sebestyen, 2011b), and concentrations may become elevated in advance of the freezing front (Kadlec, 1984; Kadlec & Li, 1990; Kadlec, Li, & Cotten, 1988; Kolka et al., 2001). Pokrovsky, Karlsson, and Giesler (2018) showed that repeated freeze–thaw cycles in Arctic peatlands can affect concentrations of trace metals and organic carbon in surface water. Freezing effects on pore water Hg have not previously been reported, but similar frost exclusion mechanisms may occur within peatlands and influence the depth distribution and concentrations of Hg.

Research on the effects of thawing on Hg often focuses on snowmelt, aboveground impacts, and peatland connectivity to downstream surface waters (Mitchell, Branfireun, & Kolka, 2008; Verry et al., 2011b). Belowground mechanisms can also provide understanding of Hg storage and release. For example, Corbett-Hains et al. (2012) showed that thawing increased the flux of Hg vapor ( $\text{Hg}^0$ ) from soil and proposed that the expansion and contraction of the soil led to the physical evacuation of  $\text{Hg}^0$  from the pore space. Freeze and thaw events have also been shown to affect nutrient release and/or retention processes due to physical disruption of soil (Matzner & Borken, 2008; Rydberg, Klaminder, Rosen, & Bindler, 2010; Yu, Zhang, Zhao, Lu, & Wang, 2010). We are not aware of previous reports of freeze–thaw effects on total mercury (THg) and MeHg concentrations in peatland pore water.

The objective of this study was to determine the effect of freezing and thawing on pore water Hg concentrations in peat columns and to provide insight into potential Hg processes occurring in peat during cold temperatures. The results provide a better understanding of current temporal biogeochemical processes within peatland ecosystems and the possible impacts from climate change. We hypothesized that ice formation would exclude THg and MeHg from saturated peat pore waters and thereby increase their concentrations in the depths below the ice front. We compared concentrations in the depths just below the freezing front with the concentrations in the lowest depths in the columns. During subsequent thawing, we hypothesized that THg and MeHg concentrations would increase throughout the peat profile. We compared concentrations collected during the freezing cycle with those from the thawing cycle.

### Core Ideas

- A freeze–thaw cycle was simulated on intact peat columns from an ombrotrophic bog.
- Novel methods were used to sample pore water in advance of the ice front and as ice melted.
- Concrete frost in peat results in higher pore water Hg concentrations below the freezing front.
- Pore water total Hg concentrations were elevated after a freeze–thaw transition.
- Methylmercury concentrations did not increase during the freeze–thaw cycle.

## 2 | MATERIALS AND METHODS

### 2.1 | Site location

We collected four large, intact columns of peat from an ombrotrophic bog on the USDA Forest Service's Marcell Experimental Forest (MEF) in north-central Minnesota. The MEF is located within the Chippewa National Forest and is 40 km north of Grand Rapids, MN. The MEF is a long-term research site that has been active since 1960 and has some of the longest-term records of northern peatland hydrology and chemistry (Kolka et al., 2011). A peatland west of the well-studied S1 bog was selected for the collection of 60-cm-tall intact columns (Figure 1). The soil is similar to the Greenwood Series: Dysic, frigid Typic Haplohemist (National Cooperative Soil Survey, 1987). This peatland is an ombrotrophic bog dominated by mature black spruce [*Picea mariana* (Mill.) Britton, Sterns & Poggenb.], ericaceous shrubs, and *Sphagnum* mosses. Soil columns were extracted within a 100-m<sup>2</sup> area in the bog hollows and away from the lag (Verry et al., 2011b).

### 2.2 | Peat column setup

In May 2015, after in situ thawing, the four peat columns were collected by pushing polyvinyl chloride columns (30 cm diameter, 60 cm tall) with beveled ends into a hollow of the bog. Because of the relatively large diameter of the columns, we did not observe any compaction within the column center, but a small amount of compression may have occurred along the column edges. We extracted each column by digging a hole next to the inserted polyvinyl chloride column, fastening a metal plate underneath the column bottom, and lifting it out of the bog. A peat column was gently placed into a 30-cm flexible end cap. All peat columns were transported to a refrigerated room at the University of Minnesota in St. Paul, MN.

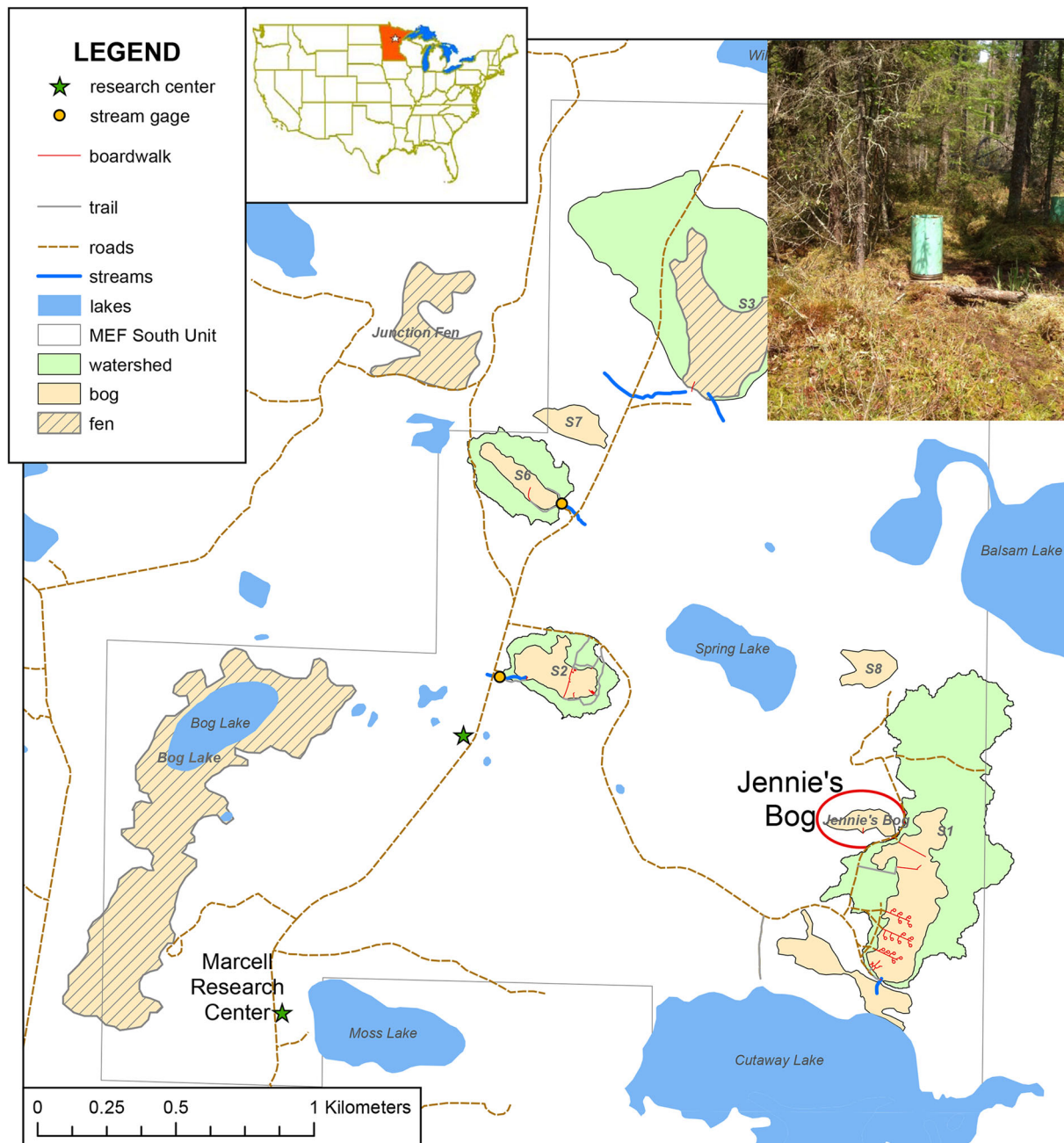


**FIGURE 1** Map of the Marcell Experimental Forest (MEF) in northern Minnesota. The study site location, Jennie's Bog, is circled in red and is west of the S1 bog. A ground photo of Jennie's Bog and a peat column is shown in the upper right corner

Sampling tubes were horizontally inserted into each column at seven depths in the peat (5, 10, 15, 20, 25, 30, and 35 cm) to establish discrete sampling depths (Figure 2). These depths were chosen to sample underneath ice during freezing and thawing. Perfluoroalkoxy (PFA) tubes were pushed through holes in clean silicone stoppers and inserted into drilled holes in the peat column sides at the sampling depths (Figure 2). The tubing had 6.4 mm outer diameter and 4.0 mm inner diameter, with 1.6-mm perforations at 1-cm increments starting 2.5 cm from the ends of the tubing. The tubing ends inside the column were heat sealed to prevent

water sampling at the column edges and to limit sampling to the column interiors. If water leaked at a silicone stopper, leaks were sealed on the outside of the column with silicone caulk and/or hydrophilic polyurethane caulk. The tubes protruding from each column depth were connected with two 6.4-mm polypropylene union tees (Figure 2). Tubing ends were capped with a removable polytetrafluoroethylene heat shrink tube and a closed end of PFA tube when water sampling was not occurring. All tubes and stoppers were cleaned for trace element sampling according to USEPA Method 1631 (Telliard & Gomez-Taylor, 2002).

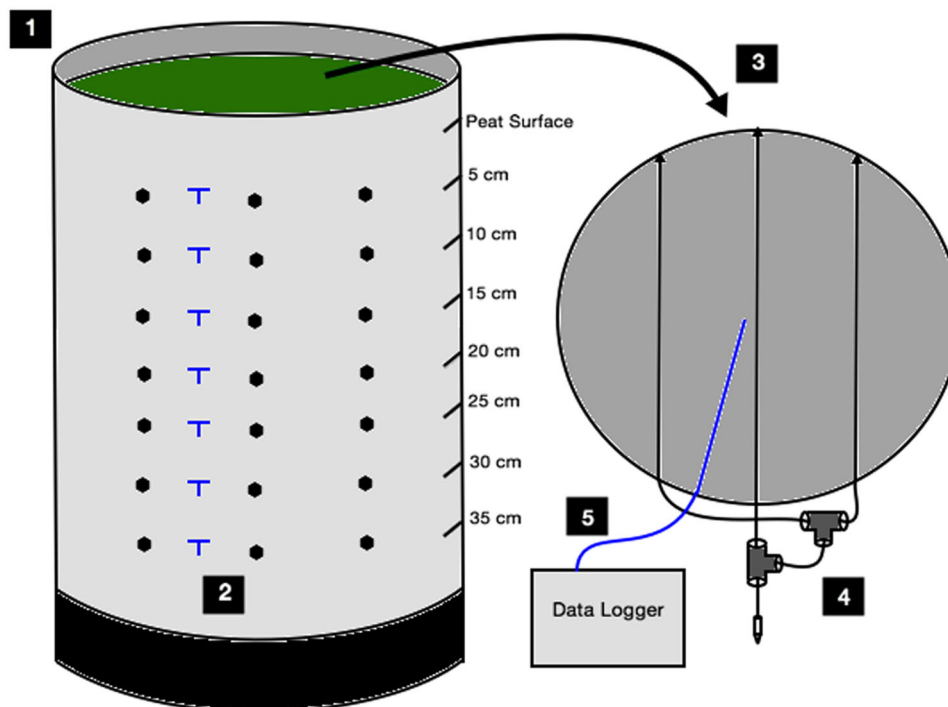


**FIGURE 2** Column setup. (1) Open column top. (2) Black circles show the locations where tubes were inserted, and blue Ts show locations of thermocouples. (3) Tubes and thermocouples were inserted at each individual layer. (4) Tube tees connected tubes from the outside and a cap on the sampling tube. (5) The blue thermocouple inside the column is connected to a data logger to record temperature

In a similar manner, thermocouples were pushed through clean silicone stoppers and inserted midway into each peat column at the various sampling depths (Figure 2). Campbell data loggers were programmed to measure temperature every 10 min from each column's sampling depths. Peat temperature was checked immediately prior to water sampling; readings below 0°C were considered frozen for sampling purposes, and readings above 0°C were considered thawed.

Two portable wooden carts were constructed to store the four peat columns during the experiment. Peat columns were fully insulated on the bottom with 41.9-cm rigid polystyrene insulation and on all sides with 11.4-cm rigid polystyrene and additional fiberglass insulation. Peat column insulation was critical for effective simulation of freezing and thawing in a laboratory setting (Nagare, Schincariol, Quinton, & Hayashi, 2012). Both freezing and thawing processes started at the top of the columns and advanced downward, as would naturally occur in the field.

### 2.3 | Experimental design

Before water sampling, we added an average of 5 L of deionized water to each 39.8 L column, which was also when water reached a depth of 2 cm above the peat surface in each column. We estimate that the pore water volume in the columns was 34.9–36.8 L based on peat having 90% porosity

(Ours, Siegel, & Glaser, 1997). The total quantity withdrawn during sampling was about 2.1 L from each column. The depths sampled changed each sampling event based on the location of the ice front. Minimal water was removed during samplings to prevent column moisture loss from influencing the results.

Sodium bromide (NaBr), a solute tracer, was added to each column by carefully distributing 50 ml of a 38.6 mg L<sup>-1</sup> NaBr solution across the surface of each column. The NaBr served as a tracer to monitor water movement by depth in the pore water of the peat columns. This tracer is nonreactive at lower concentrations and was chosen because of its low background concentration in peat and peat pore water (Baird & Gaffney, 2000; Meiri, 1989).

Temperature manipulation simulated the range of typical field temperatures and a truncated seasonal cycle. Peat columns were collected from the peatland after in situ thawing from the previous winter. In the experiment, columns were warmed, temporarily cooled, frozen, and thawed. The air temperature during the 109-d warming treatment ranged between 18 and 26°C in a greenhouse where the columns were instrumented and prepped. After warming, all columns were moved to a 53-d cooling treatment to mimic the transition into winter. Air temperatures ranged between -3 and 17°C, and the pore water was sampled once. After cooling, columns were moved into a 20-d freezing treatment where air temperature was -8°C. Pore water was sampled just below the advancing



ice front and at the bottom of the columns on three separate dates. After freezing, columns were moved to a 23-d thawing treatment at 19°C air temperature, and the pore water was sampled on three separate dates.

## 2.4 | Data collection

### 2.4.1 | Water sampling

Supplies for sampling water from columns were prepared following USEPA method 1631, including cleanroom techniques and procedures for handling samples (Telliard & Gomez-Taylor, 2002). A column depth was sampled by attaching a PFA two-port impinger to the sampling tubing. Water samples were withdrawn into a sterile 125-ml polyethylene terephthalate glycol-modified bottle using vacuum pressure. A 35-ml subsample was transferred to a clean, high-density polyethylene bottle for ion chromatography and DOC analysis. The remaining sample was preserved for Hg analysis by adding 0.25 ml of trace metal-grade concentrated hydrochloric acid. Then the preserved samples were filtered through a 47-mm, single-stage PFA filter apparatus with 0.70- $\mu\text{m}$  Whatman glass microfiber filters that had been cleaned of Hg by heating to 450°C for 90 min. The filtered samples were transferred to a sterile polyethylene terephthalate glycol-modified bottle and refrigerated until analysis.

### 2.4.2 | Chemical analysis

Filtered samples from the peat columns were analyzed for Hg in a clean laboratory at the University of Minnesota in St. Paul, MN. Total Hg concentration was measured using in-vial sparging configuration with a Tekran Model 2600 cold vapor atomic fluorescent spectrophotometry mercury analysis system according to USEPA method 1631 (Telliard & Gomez-Taylor, 2002). The detection limit for THg was 0.05 ng L<sup>-1</sup>. Quality assurance and quality control methods included analytical blanks ( $n = 17$ ), analytical standards ( $n = 20$ ), sample duplicates ( $n = 31$ ), matrix spikes ( $n = 10$ ), and standard reference materials ( $n = 4$ ). The mean and SD of matrix spike percent recoveries was  $99.4 \pm 3.7\%$ . The relative percent differences (RPDs) were <25% for 96% of THg duplicate samples. All samples of standard reference materials had percent recoveries >75%. The standard reference materials were obtained from the National Institute of Standards and Technology (2014).

Methylmercury was analyzed by capillary gas chromatography and cold vapor atomic fluorescent spectrophotometry using a Tekran Model 2700 Methyl Mercury Analyzer according to USEPA method 1630 (Telliard, 1998). The detection limit for MeHg was 0.009 ng L<sup>-1</sup>. The quality assurance and

quality control methods included analytical blanks ( $n = 21$ ), distillation blanks ( $n = 21$ ), analytical standards ( $n = 18$ ), sample duplicates ( $n = 34$ ), and matrix spikes ( $n = 8$ ). The mean  $\pm$  SD of matrix spike percent recoveries was  $130.8 \pm 81.8\%$ . All MeHg concentrations were <2.4 ng L<sup>-1</sup>, and the RPDs were <25% for over 50% of MeHg sample duplicates.

Bromide and DOC from the peat columns were analyzed at the Forestry Sciences Laboratory of the USDA Forest Service Northern Research Station in Grand Rapids, MN. Unfiltered water samples were analyzed on an ion chromatograph with a detection limit of 0.05 mg L<sup>-1</sup> for bromide, and USEPA Method 300 protocols were followed (Pfaff, 1993). Dissolved organic carbon concentration was measured on a Shimadzu TOC-LCPH combustion analyzer after samples were filtered through Whatman Grade GF/F syringe filters with 0.70  $\mu\text{m}$  pore size. The detection limit for DOC was 0.5 mg L<sup>-1</sup> and USEPA Method 415.3 protocols were followed (Potter & Wimsatt, 2005). Duplicates were analyzed every 10 samples, and the RPDs were <25% for all DOC sample duplicates.

### 2.4.3 | Bulk density

After the freeze-thaw cycle, a Russian peat corer (Jowsey, 1966) was used to take three peat samples for bulk density and von Post measurements (von Post, 1922) at the pore water sampling depths in a peat column. The three replicates were averaged to provide a mean for each depth. The von Post H-values (degree of humification) were assessed and interpreted according to Verry et al. (2011a). For bulk density, the peat was oven dried at 70°C for 72 h and calculated by dividing the oven-dry mass (g) by the volume of the sample (cm<sup>3</sup>).

### 2.4.4 | Data analysis

Columns were treated as four replicates during the experiment and throughout the analysis. The data were approximately normally distributed after testing for skewness and kurtosis. All statistical analyses were conducted in the R statistical program (R Core Team, 2016). To determine if frost exclusion occurred, we compared water chemistry concentrations in the depths just below the freezing front with those in the 25- to 35-cm depth, which were the lowest depths of the column that remained unfrozen during the experiment. An independent  $t$  test was used to determine statistically significant increases below the freezing front. All samples collected during the freezing treatment were then compared with samples collected during thawing. Water chemistry data were classified into three depth groupings (10–15, 20–30, and 35 cm) and analyzed with one-way ANOVA to determine significant concentration changes within comparable depths from

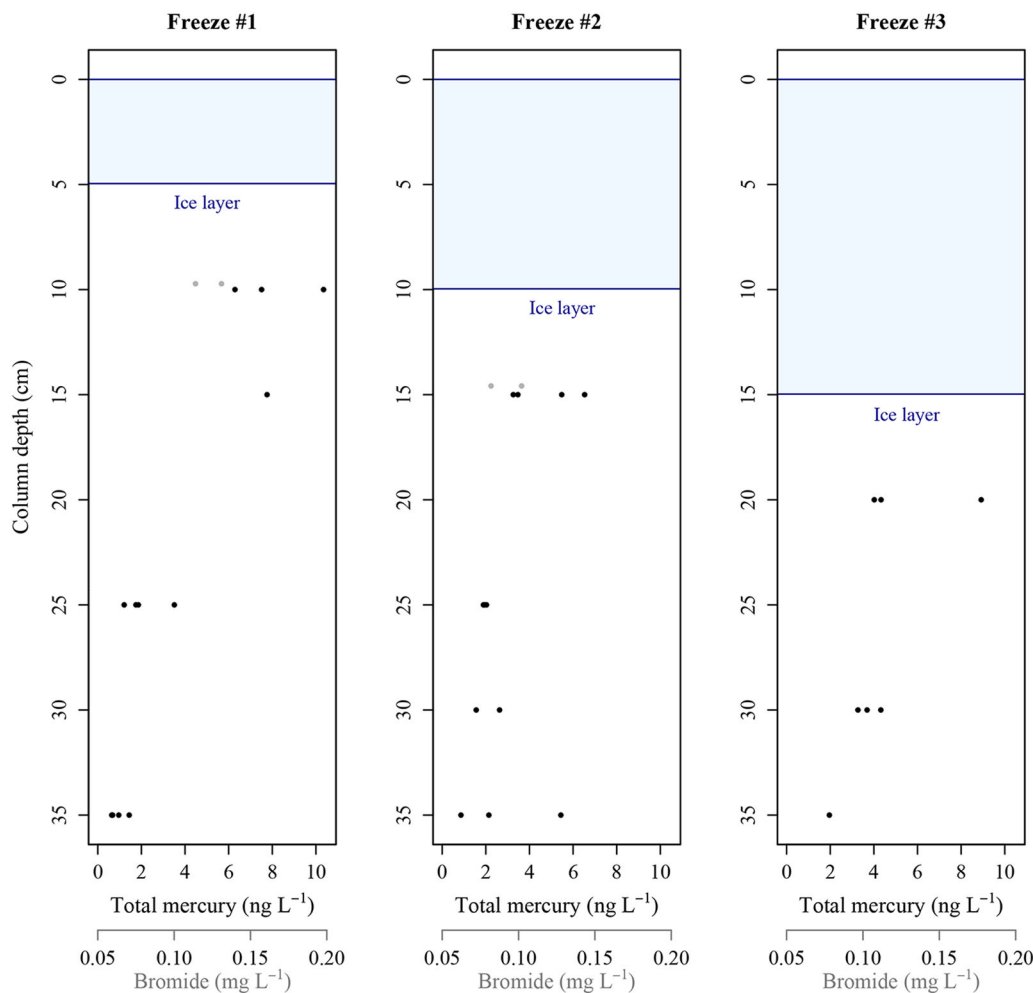


**FIGURE 3** Pore water total Hg and bromide tracer concentrations from all four columns during the three freezing treatment water samplings: Freeze #1 (12 Jan. 2016), Freeze #2 (13 Jan. 2016), and Freeze #3 (14 Jan. 2016). Total Hg results are shown in black, and bromide results are in gray (only bromide concentrations above the detection limit of 0.05 mg L<sup>-1</sup> are shown). Shaded region represents the location where peat temperature was below 0°C and approximately where the ice layer resided during that sampling date

freezing to thawing. The 5-cm depth was not sampled throughout the freeze–thaw cycle because it did not yield pore water samples after the water level dropped below that tubing depth and therefore was not included in this analysis.

Mercury has an affinity for organic matter, so Hg/DOC ratios were calculated and presented as a logarithm to provide a reasonable scale for further analysis and comparison to other published values (Mitchell et al., 2008). One-way ANOVA and Tukey's range test were used to determine if Hg/DOC ratios significantly changed within pore water during the freeze–thaw cycle.

Data from the whole freeze–thaw cycle were analyzed between sampling depths to determine how concentrations changed with depth. An overall mean  $\pm$  SD was calculated for the pore water chemistry, bulk density, and von Post H-value at each sampling depth. One-way ANOVA and Tukey's range test were used to determine if pore water chemistry significantly changed with depth.

### 3 | RESULTS

#### 3.1 | Peat column pore water chemistry during freezing

During freezing, the ice layer progressed down the column, as it does in the natural environment. The four columns had similar temperature profiles, and the lowest depth of ice formation was 15 cm.

During the cooling treatment, the pore water THg mean  $\pm$  SD at 5 and 35 cm were  $13.9 \pm 8.27$  and  $2.35 \pm 1.30$  ng L<sup>-1</sup>, respectively. When freezing began, we sampled the uppermost unfrozen depth (just below the descending ice front) and compared that with the 25- to 35-cm depths. Depth profiles of pore water chemistry show that THg was more concentrated in advance of ice in peat columns during freezing (Figure 3). The pore water THg concentration in the depth below the ice was significantly higher than pore water THg

**TABLE 1** Results for Hg. Mean concentrations below the ice layer and peat column bottom are compared by a *t* test during each freezing sampling date. Statistically significant relationships are shown with *p* values ( $p < 0.05$ )

Freezing sampling date	Location in column	Hg ng L <sup>-1</sup>	df	Significance	
				<i>t</i> test	<i>p</i> value
12 Jan. 2016					
Pore water THg <sup>a</sup>	below ice: 10 cm	8.05	2.30	−5.25	0.025
	bottom: 25–35 cm	1.51			
Pore water MeHg <sup>b</sup>	below ice: 10 cm	0.21	7.88	1.12	0.294
	bottom: 25–35 cm	0.30			
13 Jan. 2016					
Pore water THg	below ice: 15 cm	4.69	5.31	−2.56	0.048
	bottom: 25–35 cm	2.31			
Pore water MeHg	below ice: 15 cm	0.23	3.96	−0.05	0.959
	bottom: 25–35 cm	0.22			
14 Jan. 2016					
Pore water THg	below ice: 20 cm	5.76	2.40	−1.47	0.258
	bottom: 25–35 cm	3.31			
Pore water MeHg	below ice: 20 cm	0.52	1.86	−3.49	0.081
	bottom: 25–35 cm	0.16			

<sup>a</sup>Total mercury.

<sup>b</sup>Methylmercury.

concentrations at the bottom of the column during the first two freezing sampling dates ( $p < 0.05$ ) (Figure 3; Table 1). Mean pore water THg concentrations at the bottom of the columns slightly increased as freezing advanced down the column (Figure 3), but the increase at 35 cm was not significant (one-way ANOVA,  $p > 0.05$ ).

The bromide tracer at 5 cm during the cooling treatment had a mean  $\pm$  SD of  $0.15 \pm 0.09$  mg L<sup>-1</sup>. The bromide concentration in the 20- to 35-cm depths was below the detection limit of 0.05 mg L<sup>-1</sup>. As freezing began, the NaBr moved down the column with ice formation (Figure 3). There was limited solute movement past 15 cm, which was also the lowest depth of ice formation during the experiment.

During the cooling treatment, the pore water MeHg mean  $\pm$  SD values at 5 and 35 cm were  $0.02 \pm 0.02$  and  $0.43 \pm 0.26$  ng L<sup>-1</sup>, respectively. After freezing began, MeHg concentrations increased in the depth below the ice compared with the bottom of the column, but the trend was not significant ( $p > 0.05$ ) (Table 1). Concentrations of MeHg at the core bottom varied little during the freezing cycle.

### 3.2 | Peat column pore water chemistry from freeze to thaw

Pore water THg concentrations increased significantly (one-way ANOVA,  $p < 0.05$ ) from freezing to thawing (Figure 4) and at all depth groupings ( $p < 0.05$ ) (Table 2). Pore water MeHg concentrations decreased significantly at the 10- to

15-cm and the 20- to 30-cm depth groupings ( $p < 0.05$ ) from freezing to thawing (Table 2; Figure 4). In contrast to THg, the 35-cm depth showed no significant change from freezing to thawing.

Pore water DOC concentrations showed no significant changes from freezing to thawing (Table 3). Log THg/DOC ratios significantly increased from freezing to thawing at all depth groupings (Table 3). Log MeHg/DOC ratios significantly decreased from freezing to thawing at 10–15 cm (Table 3).

### 3.3 | Bulk density, von Post values, and pore water chemistry with depth

The bulk density was  $0.09$  g cm<sup>-3</sup> at 15 cm and increased to  $0.12$ – $0.13$  g cm<sup>-3</sup> below 15 cm (Table 4). The von Post values increased with each depth layer, starting at 15 cm with a von Post value of H-4 (Table 4). Mean pore water DOC concentration significantly decreased from 15 to 35 cm (one-way ANOVA,  $p < 0.05$ ) (Table 4). The DOC SD was lowest at 35 cm, which was the most frequently sampled depth. Mean THg concentrations significantly decreased from 10 to 35 cm (one-way ANOVA,  $p < 0.05$ ) (Table 4). Similar to DOC, the THg SD was lowest at 35 cm. Mean pore water MeHg concentrations were not significantly different between depths. Pore water bromide concentrations were above the detection limit at 5, 10, and 15 cm before and during freezing but below the detection limit during thawing. Mean bromide concentrations

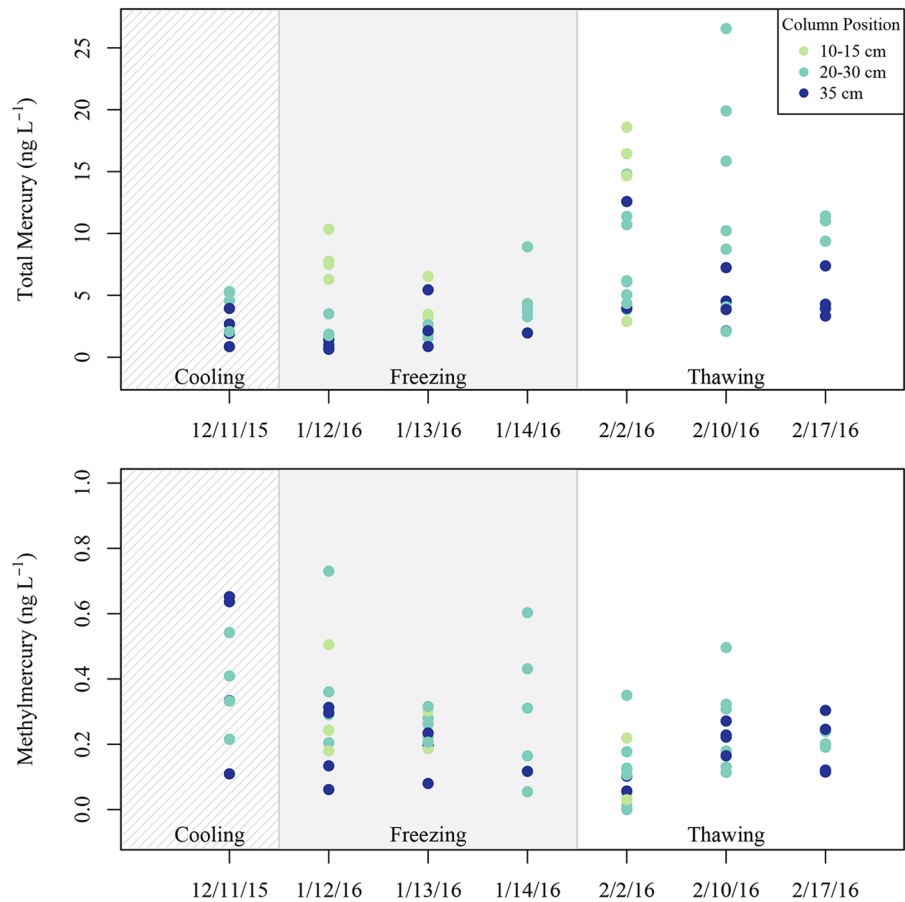


**FIGURE 4** Top graph shows total Hg pore water concentrations in all columns during each sampling date. Bottom graph shows methylmercury pore water concentrations in all columns during each sampling date. Depth groupings (10–15, 20–30, and 35 cm) are shown in three different colors, and backgrounds are shaded based on the experimental phase. The cooling treatment was used as a reference of initial concentrations, and the freezing and thawing treatments were used in the data analysis

**TABLE 2** Pore water total Hg (THg) and methylmercury (MeHg) classified into depth groupings of 10–15 cm, 20–30 cm, and 35 cm. Samples were compared between freeze and thaw using a one-way ANOVA. Statistically significant relationships are shown with *p* values (*p* < 0.05)

	Depth group	Process	<i>n</i> <sup>a</sup>	Concentration (mean ± SD)	<i>p</i> Value
THg, ng L <sup>-1</sup>	10–15 cm	freeze	8	6.33 ± 2.33	0.027
		thaw	4	13.14 ± 7.02	
	20–30 cm	freeze	15	3.13 ± 1.92	<0.001
		thaw	18	10.09 ± 6.23	
	35 cm	freeze	8	1.77 ± 1.59	0.009
		thaw	10	5.32 ± 3.03	
MeHg, ng L <sup>-1</sup>	10–15 cm	freeze	6	0.27 ± 0.12	0.036
		thaw	4	0.08 ± 0.09	
	20–30 cm	freeze	14	0.32 ± 0.18	0.017
		thaw	18	0.18 ± 0.13	
	35 cm	freeze	8	0.18 ± 0.10	0.925
		thaw	10	0.18 ± 0.08	

<sup>a</sup>Within the group being analyzed, *n* corresponds to the number of water chemistry samples being compared.



**TABLE 3** Pore water dissolved organic C (DOC), log total Hg (THg)/DOC, and log MeHg/DOC classified into depth groupings of 10–15 cm, 20–30 cm, and 35 cm within the peat columns. Samples were compared between freeze and thaw using a one-way ANOVA. Statistically significant relationships are shown with *p* values (*p* < 0.05)

	Depth group	Process	<i>n</i> <sup>a</sup>	Concentration (mean ± SD)	<i>p</i> value
DOC, mg L <sup>-1</sup>	10–15 cm	freeze	8	191 ± 39.69	0.065
		thaw	4	143 ± 32.63	
	20–30 cm	freeze	9	140 ± 39.59	0.861
		thaw	17	142 ± 29.46	
	35 cm	freeze	6	108 ± 18.19	0.136
		thaw	9	125 ± 21.64	
Log THg/DOC	10–15 cm	freeze	8	-7.50 ± 0.12	0.032
		thaw	3	-7.16 ± 0.36	
	20–30 cm	freeze	8	-7.83 ± 0.15	<0.001
		thaw	16	-7.25 ± 0.26	
	35 cm	freeze	4	-7.86 ± 0.34	0.009
		thaw	9	-7.41 ± 0.19	
Log MeHg/DOC	10–15 cm	freeze	6	-8.85 ± 0.13	0.081
		thaw	3	-9.27 ± 0.51	
	20–30 cm	freeze	8	-8.66 ± 0.18	0.103
		thaw	16	-9.37 ± 1.16	
	35 cm	freeze	4	-8.78 ± 0.28	0.524
		thaw	9	-8.89 ± 0.28	

<sup>a</sup>Within the group being analyzed, *n* corresponds to the number of water chemistry samples being compared.

**TABLE 4** Bulk density and von Post humification values determined at the end of the freeze–thaw cycle. Mean pore water chemistry for all samples during the whole experiment are reported by sampling depths. Mean ± SD was calculated at each depth for pore water dissolved organic C (DOC), bromide, total Hg (THg), and methylmercury (MeHg)

Depth cm	Bulk density g cm <sup>-3</sup>	von Post (H-value)	DOC	Bromide	THg	MeHg
			mg L <sup>-1</sup>	mg L <sup>-1</sup>	ng L <sup>-1</sup>	ng L <sup>-1</sup>
5	0.05	3	223 ± 35.74	0.12 ± 0.09	13.87 ± 8.27	0.02 ± 0.02
10	0.05	3	174 ± 45.54	0.06 ± 0.06	11.48 ± 5.11	0.12 ± 0.11
15	0.09	4	176 ± 44.89	0.05 ± 0.03	6.55 ± 4.73	0.24 ± 0.15
20	0.12	5	147 ± 42.00	0.03 ± 0.03	8.26 ± 4.27	0.25 ± 0.25
25	0.12	6	146 ± 36.54	0.02 ± 0.01	6.07 ± 6.55	0.30 ± 0.16
30	0.13	7	137 ± 28.41	0.02 ± 0.02	6.64 ± 5.12	0.21 ± 0.12
35	0.12	8	117 ± 20.78	0.01 ± 0.01	3.49 ± 2.83	0.23 ± 0.16

significantly decreased with depth from 5 to 35 cm (one-way ANOVA, *p* < 0.05) (Table 4).

## 4 | DISCUSSION

### 4.1 | Effects of freezing on peat column pore water chemistry

During freezing, pore water THg concentrations were significantly greater below the ice front than at the bottom of the column. Concentrations at the bottom of the column also increased as freezing progressed downward. These pore

water changes demonstrate THg concentrating ahead of the freezing front. When soil and water freeze solid, solutes are excluded from the ice and concentrate in the liquid water, a process known as frost exclusion (Corte, 1962; Kadlec, 1984; Kadlec et al., 1988). The increase in THg concentrations below the freezing front in column are consistent with frost exclusion. This observation is also supported by the increased concentration of NaBr tracer down the peat column during freezing (Figure 3). Solute transport was limited past 15 cm (which also coincided with maximum frost depth in the experiment), where soil bulk density increased and is likely associated with lower hydraulic conductivity in the peat. As freeze–thaw cycles change with climate change, concrete frost

formation and frost exclusion may become altered in northern peatlands.

In contrast to THg, MeHg pore water concentrations did not increase below the ice front compared with the bottom of the column. In addition, MeHg pore water concentrations fluctuated little at the column bottom. We expected limited MeHg production during cold periods (Sokolova, 2010), and neither frost exclusion nor anaerobic bacterial production appear to have affected pore water MeHg concentrations.

## 4.2 | Effects of thawing on peat column pore water chemistry

Pore water THg concentrations increased significantly throughout the peat column during the transition from freezing to thawing. This pattern of increasing concentrations during thawing has been observed in previous research in cold environments and for different water chemistries (Yu et al., 2010, 2011). We did not investigate the exact mechanisms leading to increased THg concentrations, but this type of concentration change response with frost thawing could affect Hg cycling and transport in northern peatlands.

Our study builds on other Hg field studies at the MEF, where the peat columns originated. Mitchell et al. (2008) found that spring snowmelt period accounted for 26–39% of annual THg export from the peatland watershed. Upland runoff and dry deposition can be major sources of Hg to streams that drain peatlands (Kolka, Grigal, Verry, & Nater, 1999a,b; Woerndle et al., 2018). Also, lateral runoff of bog water (Verry et al., 2011b) will similarly connect Hg from atmospheric deposition when near-surface bog water radially flows to a surrounding lagg and then to an outlet stream. Our study focused on how Hg concentration in pore waters responded within an experimental freeze–thaw cycle. The experimental design limited lateral solute migration and eliminated lateral water flow. Although this experiment is a simplified approach to assess the effects of frost exclusion on Hg concentration, the physical limitations highlight a need to further assess field conditions and Hg transport via lateral flow through peatlands.

Contrary to THg results, MeHg concentration did not increase during thawing and instead decreased significantly from freezing to thawing in the middle depths of the peat columns. One explanation for a lack of increased MeHg concentrations could be that the columns experienced a quick thaw relative to field conditions. With a steady air temperature of ~19°C, it took only 14 d for column temperatures to exceed 0°C at all depths and 23 d for the last thawing sampling to occur. In comparison, a natural spruce bog environment takes an average of 16 melting degree days to melt 1 cm of frost (Verry, 1991). Yang et al. (2016) found that increasing

the time of warming incubation of organic soil to 45–100 d at 8°C led to an accelerated MeHg production rate. Field studies have also found that MeHg concentrations are higher in late summer than in spring (Lee, Bishop, Pettersson, Iverfeldt, & Allard, 1995; Wang, Xing, Wei, & Jia, 2013). Our short thaw period with the first sampling occurring 8 d after air temperature increased was probably insufficient for MeHg concentrations to increase.

Peatlands are sources of Hg to nearby aquatic ecosystems (Driscoll et al., 1995; Kolka et al., 1999a). Mercury is mobilized with DOC, often during snowmelt or thawing periods (Kolka et al., 1999a, 2001; Mitchell et al., 2008; Schelker, Burns, Weiler, & Laudon, 2011; Shanley et al., 2002). Mercury/DOC ratios have been used to infer the source of Hg because DOC concentrations are different among landscape areas, such as uplands and peatlands (Haynes & Mitchell, 2012; Mitchell et al., 2008; Schelker et al., 2011). We measured the changes within one hydrological compartment (i.e., peat pore water) and use other studies to frame these results relative to other landscape source areas. Like Mitchell et al. (2008), we found a significant increase in THg/DOC ratio from freezing to thawing (Table 3). Likewise, we found a significant decrease in MeHg/DOC ratio during thawing at the top of the column (Table 3). Peat pore water chemistry significantly changed with the transition from freeze to thaw, suggesting the importance of studying northern peatlands during the freeze–thaw cycle.

## 4.3 | Effects from peat column depth on bulk density, von Post values, and pore water chemistry

Peat is stratified into three layers: the acrotelm, the mesotelm, and the catotelm. The acrotelm and mesotelm represent near-surface layers through which most water and solutes are laterally transported through peatlands to downstream surface water bodies (Clymo, 1984; Romanov, 1961; Verry et al., 2011b). Furthermore, ice depths at the MEF, where the cores were collected, commonly ranges up to 15 cm in depth (Verry, 1991).

The acrotelm, a surficial layer, has low bulk density and higher hydraulic conductivity than the mesotelm or catotelm (Clymo, 1984; Verry et al., 2011b). The mesotelm is a transitional layer that has slightly increased bulk density (Tfaily et al., 2014) from the acrotelm. The catotelm generally has increased bulk density from the mesotelm and much lower hydraulic conductivity than the acrotelm or mesotelm (Verry et al., 2011b). Using bulk density and von Post H-values, we identified a mesotelm layer located from 15 to 20 cm in the peat columns. Sodium bromide concentrations were all below the detection limit for depths below the mesotelm

(Figure 3), demonstrating limited solute movement past 15 cm. The decreased hydraulic conductivity of the mesotelm layer may explain the limited movement of the NaBr tracer past that depth and why THg and DOC concentrations increased little below 15 cm.

## 5 | CONCLUSIONS

Northern peatlands play a pronounced and global role in Hg-cycling processes, including local effects on downstream water quality. Understanding contemporary conditions is necessary because increasing climate temperatures could influence the duration and depth of freezing in northern peatlands and therefore change the release of Hg from peatlands. Our results support our hypothesis of increased THg concentrations in pore water below the ice front during freezing and increased concentrations throughout the peat column during thawing. However, our results did not support our MeHg hypothesis, and pore water MeHg did not significantly increase during freezing or thawing. As temperatures fluctuate with a changing climate, freeze-thaw mechanisms and other temperature-dependent processes will respond. More specifically, climate change has the potential to affect freezing length and depth due to shortened cold seasons and more frequent mid-winter thawing in peatlands. As a result, climate change could decrease the amount of time for concrete frost formation and limit THg exclusion from ice during winter months. However, climate change and effects on frost depth is highly uncertain because there is an inverse relationship between snow and frost depth. For example, more snow fall may result in less frequent and shallower concrete frost formation. Shallow concrete frost could lead to greater pore water THg concentrations at the surface because THg would no longer migrate to depths deep in the peat profile from ice formation. Studying the freeze-thaw cycle is important because we know that changes to the climate will affect Hg cycling and possible transport processes during freezing and thawing in northern peatland environments.

## ACKNOWLEDGMENTS

The Northern Research Station (NRS) of the USDA Forest Service funds the long-term monitoring and research program at the Marcell Experimental Forest. The NRS also funded this research as well as the contributions of RKK and SDS, and the Grand Rapids Forestry Sciences Chemistry Laboratory. Funding for the senior author was provided by the Graduate School and the College of Food, Agricultural, and Natural Resource Sciences, University of Minnesota. We thank Sona Psarska, Kalei Holt, and John Larson for water sample analysis and Matt Erickson, Andrew Scobbie, and John Baker for equipment, advice, and the use of their research space.


## CONFLICT OF INTEREST

The authors declare no conflict of interest.

## ORCID

Jennie I. Sirota  <https://orcid.org/0000-0002-1287-638X>

Randall K. Kolka  <https://orcid.org/0000-0002-6419-8218>

Stephen D. Sebestyen  <https://orcid.org/0000-0002-6315-0108>

## REFERENCES

- Baird, A. J., & Gaffney, S. W. (2000). Solute movement in drained fen peat: A field tracer study in a Somerset (UK) wetland. *Hydrological Processes*, 14, 2489–2503. [https://doi.org/10.1002/1099-1085\(20001015\)14:14<2489::AID-HYP110>3.0.CO;2-Q](https://doi.org/10.1002/1099-1085(20001015)14:14<2489::AID-HYP110>3.0.CO;2-Q)
- Branfireun, B. A., Roulet, N. T., Kelly, C. A., & Rudd, W. M. (1999). In: Situ sulphate stimulation of mercury methylation in a boreal peatland: Toward a link between acid rain and methylmercury contamination in remote environments. *Global Biogeochemical Cycles*, 13(3), 743–750. <https://doi.org/10.1029/1999GB900033>
- Celo, V., Lean, D. R. S., & Scott, S. L. (2006). Abiotic methylation of mercury in the aquatic environment. *Science of the Total Environment*, 368, 126–137. <https://doi.org/10.1016/j.scitotenv.2005.09.043>
- Clymo, R. S. (1984). The limits to peat bog growth. *Philosophical Transactions of the Royal Society of London*, 303(1117), 605–654. <https://doi.org/10.1098/rstb.1984.0002>
- Corbett-Hains, H., Walters, N. E., & Van Heyst, B. J. (2012). Evaluating the effects of sub-zero temperature cycling on mercury flux from soils. *Atmospheric Environment*, 63, 102–108. <https://doi.org/10.1016/j.atmosenv.2012.09.047>
- Corte, A. E. (1962). Vertical migration of particles in front of a moving freezing plane. *Journal of Geophysical Research*, 67(3), 1085–1090. <https://doi.org/10.1029/JZ067i003p01085>
- Driscoll, C. T., Blette, V., Yan, C., Schofield, C. L., Munson, R., & Holsapple, J. (1995). The role of dissolved organic carbon in the chemistry and bioavailability of mercury in remote Adirondack lakes. *Water, Air, & Soil Pollution*, 80, 499–508. <https://doi.org/10.1007/BF01189700>
- Driscoll, C. T., Mason, R. P., Chan, H. M., Jacob, D. J., & Pirrone, N. (2013). Mercury as a global pollutant: Sources, pathways, and effects. *Environmental Science & Technology*, 47, 4967–4983.
- Gilmour, C. C., & Henry, E. A. (1991). Mercury methylation in aquatic systems affected by acid deposition. *Environmental Pollution*, 71, 131–169.
- Haynes, K. M., & Mitchell, C. P. J. (2012). Inter-annual and spatial variability in hillslope runoff and mercury flux during spring snowmelt. *Journal of Environmental Monitoring*, 14, 2083–2091.
- Hodgkins, S. B., Tfaily, M. M., McCalley, C. K., Logan, T. A., Crill, P. M., Saleska, S. R., ... Chanton, J. P. (2014). Changes in peat chemistry associated with permafrost thaw increase greenhouse gas production. *Proceedings of the National Academy of Sciences*, 111(16), 5819–5824.
- Jones, D. S., Walker, G. M., Johnson, N. W., Mitchell, C. P. J., Coleman Wasik, J. K., & Bailey, J. V. (2019). Molecular evidence for novel mercury methylating microorganisms in sulfated impacted lakes. *ISME Journal*, 13(7), 1659–1675. <https://doi.org/10.1038/s41396-019-0376-1>
- Jowsey, P. C. (1966). An improved peat sampler. *New Phytologist*, 65(2), 245–248. <https://doi.org/10.1111/j.1469-8137.1966.tb06356.x>

- Kadlec, R. H. (1984). Freezing-induced vertical solute movement in peat. *Proceedings of the International Peat Congress*, 7(4), 248–262.
- Kadlec, R. H., & Li, X. M. (1990). Peatlands ice/water quality. *Wetlands*, 10(1), 93–106. <https://doi.org/10.1007/BF03160826>
- Kadlec, R. H., Li, X. M., & Cotten, G. B. (1988). Modeling solute segregation during freezing of peatland waters. *Water Resources Research*, 24(2), 219–224. <https://doi.org/10.1029/WR024i002p00219>
- Kolka, R. K., Grigal, D. F., Nater, E. A., & Verry, E. S. (2001). Hydrologic cycling of mercury and organic carbon in a forested upland-bog watershed. *Soil Science Society of America Journal*, 65, 897–905.
- Kolka, R. K., Grigal, D. F., Verry, E. S., & Nater, E. A. (1999a). Mercury and organic carbon relationships in streams draining forested upland/peatland watersheds. *Journal of Environmental Quality*, 28(3), 766–775. <https://doi.org/10.2134/jeq1999.00472425002800030006x>
- Kolka, R. K., Mitchell, C. P. J., Jeremiason, J. D., Hines, N. A., Grigal, D. F., Engstrom, D. R., ... Cotner, J. B. (2011). Mercury cycling in peatland watersheds. In R. K. Kolka (Eds.), et al., *Peatland biogeochemistry and watershed hydrology at the Marcell Experimental Forest* (pp. 349–370). Boca Raton, FL: CRC Press.
- Kolka, R. K., Nater, E. A., Grigal, D. F., & Verry, E. S. (1999b). Atmospheric inputs of mercury and organic carbon into a forested upland/bog watershed. *Water, Air, & Soil Pollution*, 113(1), 273–294.
- Lee, Y. H., Bishop, K., Pettersson, C., Iverfeldt, A., & Allard, B. (1995). Subcatchment output of mercury and methylmercury at Svartberget in northern Sweden. *Water, Air, & Soil Pollution*, 80, 455–465.
- Matzner, E., & Borken, W. (2008). Do freeze-thaw events enhance C and N losses from soils of different ecosystems? A review. *European Journal of Soil Science*, 59(2), 274–284. <https://doi.org/10.1111/j.1365-2389.2007.00992.x>
- Meiri, D. (1989). *A tracer test for detecting cross contamination along a monitoring well column* (pp. 78–81). Ground Water Monit. Rem. (Spring). <https://doi.org/10.1111/j.1745-6592.1989.tb01142.x>
- Mitchell, C. P. J., Branfireun, B. A., & Kolka, R. K. (2008). Total mercury and methylmercury dynamics in upland-peatland watersheds during snowmelt. *Biogeochemistry*, 90, 225–241. <https://doi.org/10.1007/s10533-008-9246-z>
- Morel, F. M. M., Kraepiel, A. M. L., & Amyot, M. (1998). The chemical cycle and bioaccumulation of mercury. *Annual Review of Ecology and Systematics*, 29, 543–566. <https://doi.org/10.1146/annurev.ecolsys.29.1.543>
- Nagare, R. M., Schincariol, R. A., Quinton, W. L., & Hayashi, M. (2012). Moving the field into the lab: Simulation of water and heat transport subarctic peat. *Permafrost and Periglacial Processes*, 23, 237–243. <https://doi.org/10.1002/ppp.1746>
- National Cooperative Soil Survey. (1987). *Soil Survey of Itasca County, Minnesota*. Washington, DC: Greenwood Series. USDA. Retrieved from [www.nrcs.usda.gov/Internet/FSE\\_MANUSCRIPTS/minnesota/MN061/0/Itasca\\_MN.pdf](http://www.nrcs.usda.gov/Internet/FSE_MANUSCRIPTS/minnesota/MN061/0/Itasca_MN.pdf) (accessed 29 Dec. 2018).
- National Institute of Standards and Technology. (2014). *Standard reference material: Mercury in water*. Washington, DC: United States Department of Commerce. Retrieved from [www-s.nist.gov/msrms/certificates/1641e.pdf](http://www-s.nist.gov/msrms/certificates/1641e.pdf)
- Ours, D. P., Siegel, D. I., & Glaser, P. H. (1997). Chemical dilution and the dual porosity of humified bog peat. *Journal of Hydrology*, 196(1–4), 348–360. [https://doi.org/10.1016/S0022-1694\(96\)03247-7](https://doi.org/10.1016/S0022-1694(96)03247-7)
- Pfaff, J. D. (1993). *Method 300: Determination of inorganic anions by ion chromatography*. Washington, DC: USEPA.
- Pokrovsky, O. S., Karlsson, J., & Giesler, R. (2018). Freeze-thaw cycles of Arctic thaw ponds remove colloidal metals and generate low-molecular-weight organic matter. *Biogeochemistry*, 137(3), 321–336. <https://doi.org/10.1007/s10533-018-0421-6>
- Potter, B. B., & Wimsatt, J. C. (2005). *Method 415.3: Measurement of total organic carbon, dissolved organic carbon and specific UV absorbance at 254 nm in source water and drinking water*. Washington, DC: USEPA.
- R Core Team. (2016). *R: A language and environment for statistical computing*. Vienna, Austria: R Foundation for Statistical Computing.
- Romanov, V. V. (1961). *Hydrophysics of bogs (Gidrofizika bolot)*. Israel Program for Scientific Translations, 1968. Washington, DC: USDA.
- Rydberg, J., Klaminder, J., Rosen, P., & Bindler, R. (2010). Climate driven release of carbon and mercury from permafrost mires increases mercury loading to subarctic lakes. *Science of the Total Environment*, 208, 4778–4783.
- Schelker, J., Burns, D. A., Weiler, M., & Laudon, H. (2011). Hydrological mobilization of mercury and dissolved organic carbon in a snow-dominated, forested watershed: Conceptualization and modeling. *Journal of Geophysical Research*, 116(G1), G01002.
- Sebestyen, S. D., Dorrance, C., Olson, D. M., Verry, E. S., Kolka, R. K., Elling, A. E., & Kyllander, R. (2011). Long-term monitoring sites and trends at the Marcell Experimental forest. In R. K. Kolka (Eds.), et al., *Peatland biogeochemistry and watershed hydrology at the Marcell experimental forest* (pp. 15–71). Boca Raton, FL: CRC Press.
- Shanley, J. B., Schuster, P. F., Reddy, M. M., Roth, D. A., Taylor, H. E., & Aiken, G. R. (2002). Mercury on the move during snowmelt in Vermont. *Transactions of the American Geophysical Union*, 83(5), 45–48.
- Skylberg, U., Xia, K., Bloom, P. R., Nater, E. A., & Bleam, W. F. (2000). Binding of mercury(II) to reduced sulfur in soil organic matter along upland-peat soil transects. *Journal of Environmental Quality*, 29, 855–865. <https://doi.org/10.2134/jeq2000.00472425002900030022x>
- Sokolova, E. A. (2010). Influence of temperature on development of sulfate-reducing bacteria in the laboratory and field in winter. *Contemporary Problems of Ecology*, 3(6), 631–634.
- Telliard, W. A. (1998). *Method 1630: Methyl mercury in water by distillation, aqueous ethylation, purge and trap, and cold vapor atomic fluorescence spectrometry*. Washington, DC: USEPA.
- Telliard, W. A., & Gomez-Taylor, M. (2002). *Method 1631, Revision E: Mercury in water by oxidation, purge and trap, and cold vapor atomic fluorescence spectrometry*. Washington, DC: USEPA.
- Tfaily, M. M., Cooper, W. T., Kostka, J. E., Chanton, P. R., Schadt, C. W., Hanson, P. J., ... Chanton, J. P. (2014). Organic matter transformation in the peat column at Marcell experimental forest: Humification and vertical stratification. *Journal of Geophysical Research: Biogeosciences*, 119, 661–675.
- Trimble, G. R., Sartz, R. S., & Pierce, R. S. (1958). How type of soil frost affects infiltration. *Journal of Soil and Water Conservation*, 13, 81–82.
- Verry, E. S. (1991). Concrete frost in peatlands and mineral soils: Northern Minnesota. In D. N. Grubich & T. J. Malterer (Eds.), *Peat and peatlands: The source and its utilization. Proceedings of the International Peat Symposium, Duluth, MN. 9–23 Aug. 1991* (pp. 121–141). Jyväskylä, Finland: International Peat Society.
- Verry, E. S., Boelter, D. H., Paivanen, J., Nichols, D. S., Malterer, T., & Gafni, A. (2011a). Physical properties of organic soils. In R. K. Kolka et al. (Eds.), *Peatland biogeochemistry and watershed hydrology at the Marcell experimental forest* (pp. 135–176). Boca Raton, FL: CRC Press.

- Verry, E. S., Brooks, K. N., Nichols, D. S., Ferris, D. R., & Sebestyen, S. D. (2011b). Watershed hydrology. In R. K. Kolka & S. Sebestyen (Eds.), *Peatland biogeochemistry and watershed hydrology at the Marcell experimental forest* (pp. 193–212). Boca Raton, FL: CRC Press.
- von Post, L. (1922). Sveriges geologiska undersöknings torvinvenstering och några av dess hittills vaanna resultat. *Svenska Mosskulturforen. Tidskr.*, 36, 1–27.
- Wang, S., Xing, D., Wei, Z., & Jia, Y. (2013). Spatial and seasonal variations in soil and river water mercury in a boreal forest, Changbai Mountain, Northeastern China. *Geoderma*, 206, 123–132. <https://doi.org/10.1016/j.geoderma.2013.04.026>
- Woerndle, G. E., Tsz-Ki Tsui, M., Sebestyen, S. D., Blum, J. D., Nie, X., & Kolka, R. K. (2018). New insights on ecosystem mercury cycling revealed by stable isotopes of mercury in water flowing from a headwater peatland catchment. *Environmental Science & Technology*, 52(4), 1854–1861. <https://doi.org/10.1021/acs.est.7b04449>
- Xia, K., Skjellberg, U. L., Bleam, W. F., Bloom, P. R., Nater, E. A., & Helmke, P. A. (1999). X-ray absorption spectroscopic evidence for the complexation of Hg(II) by reduced sulfur in soil humic substances. *Environmental Science & Technology*, 33, 257–261.
- Yang, Z., Fang, W., Lu, X., Sheng, G. P., Graham, D. E., Liang, L., ... Gu, B. (2016). Warming increases methylmercury production in an Arctic soil. *Environmental Pollution*, 214, 504–509. <https://doi.org/10.1016/j.envpol.2016.04.069>
- Yu, X. (2013). *Material cycling of wetland soils driven by freeze-thaw effects*. Heidelberg, Berlin: Springer. <https://doi.org/10.1007/978-3-642-34465-7>
- Yu, X., Zhang, Y., Zhao, H., Lu, X., & Wang, G. (2010). Freeze-thaw effects on sorption/desorption of dissolved organic carbon in wetland soils. *Chinese Geographical Science*, 20(3), 209–217. <https://doi.org/10.1007/s11769-010-0209-7>
- Yu, X., Zou, Y., Jiang, M., Lu, X., & Wang, G. (2011). Response of soil constituents to freeze thaw cycles in wetland soil solution. *Soil Biology and Biochemistry*, 43(6), 1308–1320. <https://doi.org/10.1016/j.soilbio.2011.03.002>

**How to cite this article:** Sirota JI, Kolka RK, Sebestyen SD, Nater EA. Mercury dynamics in the pore water of peat columns during experimental freezing and thawing. *J. Environ. Qual.* 2020;49:404–416. <https://doi.org/10.1002/jeq2.20046>